

Transient and Steady-State Magnetic Fields Induce Increased Fluorodeoxyglucose Uptake in the Rat Hindbrain

CLIFTON FRILOT II,¹ SIMONA CARRUBBA,² AND ANDREW A. MARINO^{2*}

¹*School of Allied Health Professions, Louisiana State University Health Sciences Center, Shreveport, Louisiana*

²*Department of Orthopaedic Surgery, Louisiana State University Health Sciences Center, Shreveport, Louisiana*

KEY WORDS small animal imaging; electromagnetic fields; nonlinear analysis; cerebellum; evoked potentials; PET

ABSTRACT We inquired into the biophysical basis of the ability of weak electromagnetic fields (EMFs) to trigger onset and offset evoked potentials, and to produce steady-state changes in the electroencephalogram (EEG). Rats were exposed to a 2.5-G, 60-Hz magnetic field and the neuroanatomical region of glucose activation associated with the effect of the field on the EEG was identified by positron emission tomography (PET) using fluorodeoxyglucose (FDG). Paired emission scans from the same animal with and without field treatment were differenced and averaged, and *t* values of the brain voxels computed using the pooled standard deviation were compared with a calculated critical *t* value to identify the field-activated voxels. Increased glucose utilization occurred in hindbrain voxels when the field was applied orthogonally to the sagittal plane, but not when the angle between the field and the sagittal plane varied randomly. Distinct FDG activation effects were observed in response to transient (both onset and offset) and steady-state magnetic stimuli. Observations of increased glucose utilization induced by magnetic stimuli and its dependence on the direction of the field suggested that signal transduction was mediated by a force detector and that the process and/or early posttransduction processing occurred in the hindbrain. **Synapse** 65:617–623, 2011. © 2010 Wiley-Liss, Inc.

INTRODUCTION

Humans can detect weak electromagnetic fields (EMFs), as assessed on the bases of their ability to exhibit onset and offset evoked potentials, and steady-state changes in brain electrical activity while the stimulus is present (Carrubba et al., 2007; Marino et al., 2010). Increased neuronal activity is associated with increased energy metabolism (Pizzagalli et al., 2003), so the transient and steady-state changes in brain electrical activity were presumably mediated by increased glucose utilization. Rats exhibited a magnetic sense similar to that of humans, and signal transduction was accompanied by increased uptake of fluorodeoxyglucose (FDG), as determined by PET (Frilot et al., 2009).

We proposed that the biophysical basis of EMF transduction was a force on a glycolyx molecule attached to the gate of a calcium-ion channel in the membrane of a specialized electroreceptor cell (Marino et al., 2009). In this view the component of the force along a structurally significant molecular

axis alters the probability of the ion channel to be in the open state, resulting in signal transduction. The hypothesized process is energetically possible even for low-strength EMFs (Kolomytkin et al., 2007).

Our aim here was to test whether EMF transduction was dependent on the direction of the field, and whether the previously reported EMF effects on FDG uptake actually consisted of distinct but related effects. In experiments where each rat served as its own control, we compared the FDG levels voxel by voxel in the presence and absence of EMFs to detect EMF-induced increased glucose utilization and determine whether it consisted of distinct effects associ-

*Correspondence to: Andrew A. Marino, PhD, Department of Orthopaedic Surgery, LSU Health Sciences Center, P.O. Box 33932, Shreveport, LA 71130-3932, USA. E-mail: amarino@lsuhsc.edu

Received 24 August 2010; Accepted 21 October 2010

DOI 10.1002/syn.20882

Published online 16 November 2010 in Wiley Online Library (wileyonlinelibrary.com).

ated with transient and steady-state characteristics of the EMF stimulus, and to assess whether the effect due to transient fields depended on the direction of the field, as predicted by our model of signal transduction.

MATERIALS AND METHODS

Animal exposure

Female Sprague-Dawley rats, approximately 300 g, were exposed in a darkened room to a 60-Hz magnetic field having a root mean square strength of 2.5 G (250 μ T). Fields of comparable strength occur in the general environment; those used in magnetic resonance imaging or transcranial stimulation are three to four orders larger.

We passed a computer-controlled current through a multiturn square coil to produce the applied field, which was uniform to within 10% throughout the region occupied by the rats; the coil was dipped in epoxy to guard against the possibility of vibration. The rise- and fall-times of the field (the aspects of the field that produce onset and offset evoked potentials) were about 10 ms. The rats were not aware of the presence of the field, as determined qualitatively based on the absence of behavioral responses when it was turned on or off. The equipment that generated and controlled the magnetic field produced no auditory or visual clues, and was located outside the room where the rat was located. The background 60-Hz magnetic field (present when no experimental magnetic field was applied) was 0.1 mG (0.01 μ T).

In the first experiment the rats were constrained so that the field was applied coronally, orthogonal to the sagittal plane. Prior to the experimental session, each rat was accommodated to the constraint device by means of once-a-day practice sessions until the device was accepted with no manifestations of discomfort (three to five sessions). In the second experiment each rat was free to roam in the cage during field exposure, resulting in a random vector relation between the field and the long axis of the rat. Separate groups of 10 rats were used in the two experiments.

Data acquisition

The rats were injected within 15 s (injection volume, 0.5 ml) in the tail vein with 11 MBq ($\pm 10\%$) of 18 F-labeled FDG; either magnetic-field or sham-field exposure commenced immediately thereafter and continued for 45 min. In the first experiment, each rat was injected and scanned three times: once after field exposure using a 100% duty cycle (field on at $t = 0$, off at $t = 45$ min), once using a 50% duty cycle (on for 2 s, off for 2 s repetitiously for 45 min), and once after sham-field exposure (control) for 45 min. In the second experiment the rats were injected and scanned twice, once after field exposure for 45 min using a

50% duty cycle and once after sham exposure. The minimum time between injections was two days; in both experiments the order of the exposure conditions was counterbalanced.

Immediately following field exposure or sham exposure the rats were anesthetized (5% isoflurane) and PET scans were obtained within 15 min (Concorde microPET, Knoxville, TN). The sinograms were corrected for scattered radiation and attenuation, and images were generated using a standard filtered back-projection algorithm. The image matrices were 128×128 pixels with a pixel size of 0.85×0.85 mm²; the spatial resolution in the axial direction was 1.21 mm (63 pixels).

Data analysis

The images were aligned (12-parameter affine transformation, with the normalized mutual information as the cost function), spatially normalized to the average of all the scans in the experiment, smoothed in all dimensions (full-width at half-maximum, 2 mm), and cropped to isolate brain regions (SPM, Matlab, Mathworks, Natick, MA). Paired exposed and control images were subtracted to form difference images which were averaged across all the rats in the experiment to create a mean difference image (MDI) (Shimoji et al., 2004; Worsley et al., 1992). This procedure resulted in two MDIs in the first experiment, corresponding to the 50% and 100% duty-cycle exposure conditions, and one MDI in the second experiment.

The pooled standard deviation was determined and used to compute a three-dimensional distribution in which each voxel was represented by a t value, resulting in a brain t map $T(\mathbf{x})$, where \mathbf{x} is the voxel coordinates. Voxels activated by field exposure were identified by locating the values in $T(\mathbf{x})$ that were greater than the critical t value, namely the value for which $P(t_{\max} > t) = R(4 \log_c(2))^{3/2} (2\pi)^{-2} (t^2 - 1)e^{-t^2/2}$, where R is the number of resolution elements in the search volume (4088 mm³) divided by the product of the full widths at half maximum along the three imaging axes (Worsley et al., 1992). For our MDIs $R = 510$ elements, which resulted in a critical t value of 4.697. The Euler characteristic of the distribution of activated voxels was used to estimate the number of isolated regions of activation (Worsley et al., 1992).

The anatomical locations of the statistically significant voxels were identified by localizing them in a rat magnetic resonance (MR) brain atlas (Schweinhardt et al., 2003). The process of superimposing the emission data on the MR dataset was repeated five times and the variation in placement of a representative voxel (mean \pm SD) from the emission scan on its corresponding MR voxel was 1.4 ± 0.9 mm, measured along the superior/inferior axis. Thus there was an in-

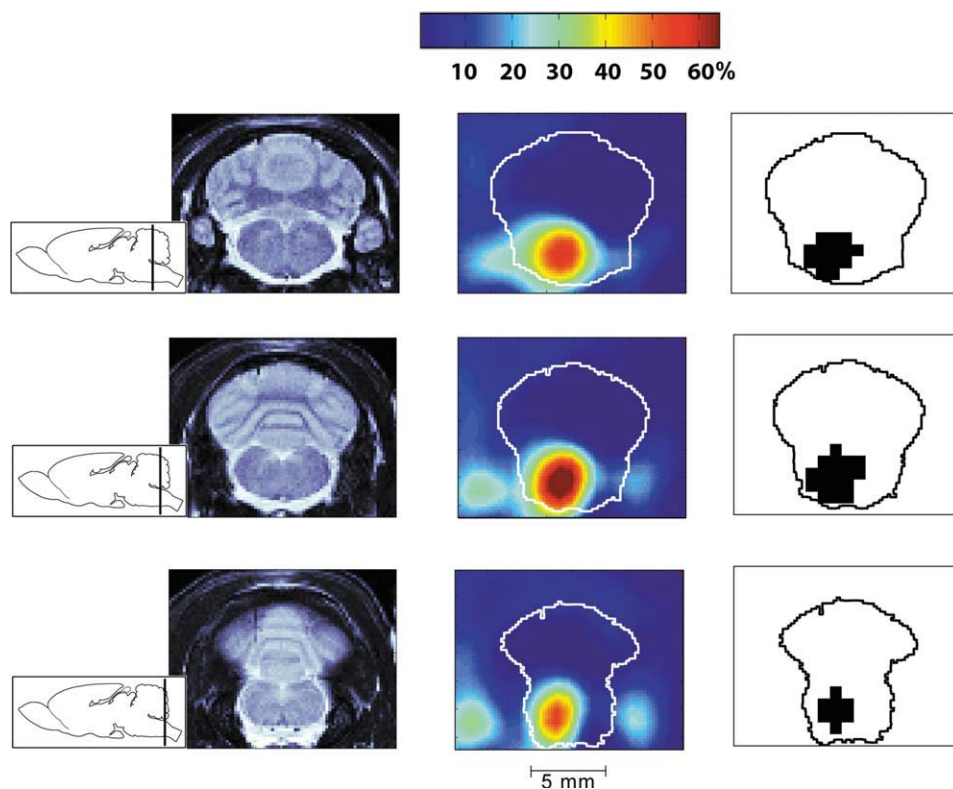


Fig. 1. Increased FDG uptake in the rat hindbrain produced by a magnetic field having a duty cycle of 50%. The activated voxels ($P < 0.05$) were located in the mid-sagittal region and occurred in three consecutive PET slices (locations shown in the inserts). First column, coronal magnetic resonance (MR) sections of the rat brain (Schweinhart et al., 2003); slice thickness, 1.2 mm. Second column, average

difference PET image ($n = 10$ rats) (superimposed outlines from MR atlas). Third column, locations in the image plane of the voxels activated by the magnetic field. Color bar for the difference image is expressed as a percent difference between the average exposure and sham-exposure PET images. Voxel dimension 0.845×0.845 mm. Caudal view. Field applied orthogonal to the plane of the section.

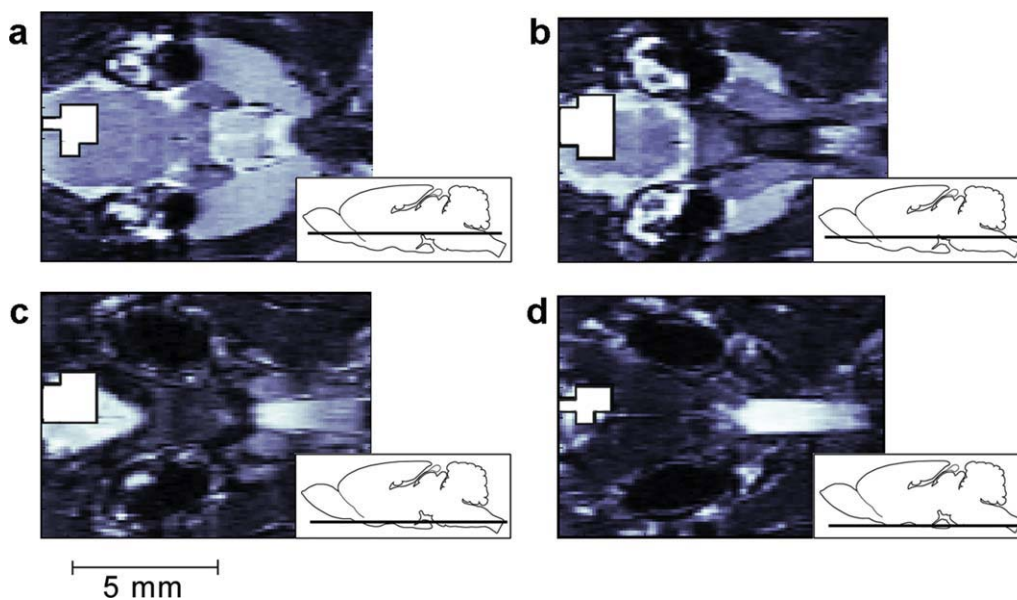


Fig. 2. Increased FDG uptake in the rat hindbrain produced by a magnetic field having a duty cycle of 50%. Consecutive transverse MR atlas slices (a through d), 0.85 mm thick (Schweinhart et al., 2003). The activated voxels ($P < 0.05$) are outlined in black. Voxel dimension 0.845×1.21 mm². Dorsal view. Field applied in the plane of the section.

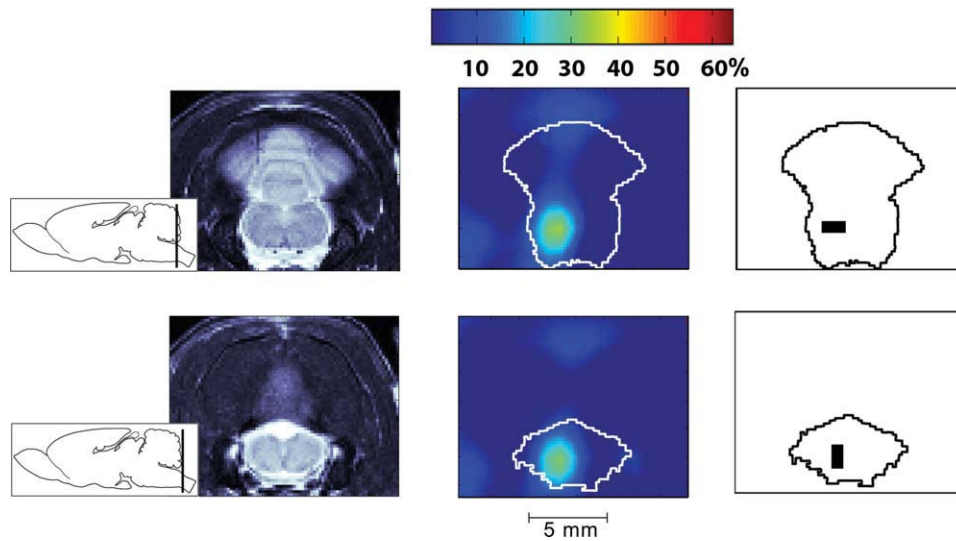


Fig. 3. Increased FDG uptake in the rat hindbrain produced by a 60-Hz magnetic field having a duty cycle of 100%. The activated voxels ($P < 0.05$) were located in the midsagittal region and occurred in two consecutive PET slices (locations shown in the inserts). First column, coronal magnetic resonance (MR) sections of the rat brain (Schweinhart et al., 2003); slice thickness, 1.2 mm. Second column, average

difference PET image ($n = 10$ rats) (superimposed outlines from MR atlas). Third column, locations in the image plane of the voxels activated by the magnetic field. Color bar for the difference image is expressed as a percent difference between the average exposure and sham-exposure PET images. Voxel dimension $0.845 \times 0.845 \text{ mm}^2$. Caudal view. Field applied orthogonal to the plane of the section.

herent error of about 2.3 mm (mean + SD) in ascertaining the anatomical location of the activated voxels.

As a negative control for the analysis, the normalized voxel values were randomized prior to forming the MDIs and then evaluated as previously, resulting in a determination of a critical value of t . The process was repeated 100 times to assess the empirical probability that the critical t value calculated from the experimental data could have been achieved by chance.

RESULTS

When the rats were constrained so that the angle between the field and the rat's body axis was fixed, fields having a duty cycle of 50% and (to a lesser extent) 100% both stimulated FDG uptake in the hind-

brain (Figs. 1–4). The respective standard deviations pooled over the search volume for the 50% and 100% duty-cycle scans were 24.4% and 23.0%; the respective maximum t values were 8.18 and 5.05. In the 50% duty-cycle MDI the activated region consisted of 31 voxels (26.8 mm^3), with an Euler characteristic of 1 and no holes in the excursion set, indicating one isolated region of activation (Figs. 1 and 2). The 100% duty-cycle MDI yielded an activated region of four voxels (3.5 mm^3) with no holes in the excursion set (Figs. 3 and 4). The average percent change in FDG uptake \pm SD in the activated voxels was $53.4 \pm 8.5\%$ and $33.9 \pm 1.2\%$ for the 50% and 100% MDIs, respectively. By comparing the location of the activated voxels in the PET image with a standard MR atlas of the rat brain (Schweinhart et al., 2003), the activated regions were located in the hindbrain (Figs. 1–4).

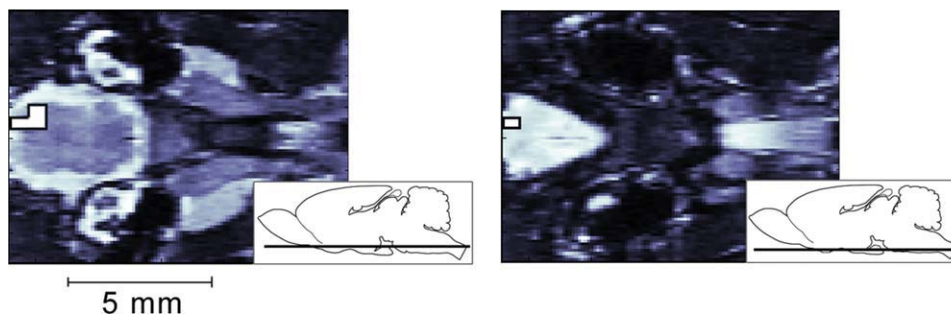


Fig. 4. Increased FDG uptake in the rat hindbrain produced by a 60-Hz magnetic field having a duty cycle of 100%. Consecutive transverse MRI atlas slices, 0.85 mm thick (Schweinhart et al., 2003). The activated voxels ($P < 0.05$) are outlined in black. Voxel dimension $0.845 \times 1.21 \text{ mm}^2$. Dorsal view. Field applied in the plane of the section.

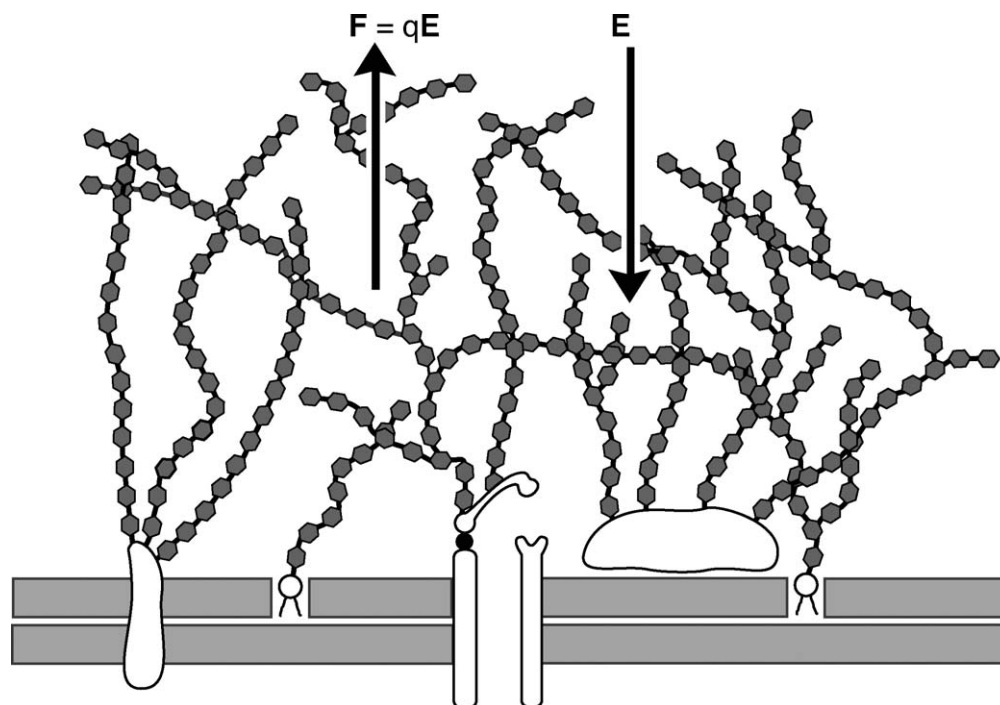


Fig. 5. Model for detection of electric fields. The glyocalyx consists of oligosaccharide side chains covalently bound to adsorbed and transmembrane proteins, including ion channels. An applied electric field E exerts a force F on the negatively charged glyocalyx molecules bound to the gate or interleaved with the bound molecules, thereby mechanically opening the channel gate.

To confirm the reliability of the analysis, the voxel values were randomized prior to formation of the difference image. During 100 iterations the critical value of 4.65 was never achieved in either of the two control MDIs when the angle between the field and the rat's body axis varied randomly.

In the second experiment the standard deviation pooled over the search volume was 26.7%, but $t < 4.697$ for all voxels indicating the absence of FDG activation by the field. The average percent change \pm SD over the 31 voxels that were activated in the 50% duty-cycle exposure was $-13.3 \pm 8.8\%$.

DISCUSSION

Separate brain networks mediate onset and offset responses to stimuli as well as responses that occur after the transient effects have ended (referred to here as steady-state responses) (Pratt et al., 2008; Yamashiro et al., 2009). Presumably each response requires increased glucose utilization. We proposed that transduction of EMFs was mediated by a directionally specific force exerted by the induced electric field on the gate of an ion channel (Kolomytkin et al., 2007). Our goal here was to detect increased FDG uptake in the brain due to magnetic stimulation under conditions that would support our biophysical theory of EMF transduction.

When the rats were exposed to a magnetic field having a duty cycle of 50% they experienced 45 min \times 60 s \div 2 s per stimulus epoch = 1350 stimulus periods resulting in a total (onset + offset) of 2700 evoked potentials that, by hypothesis, were each accompanied by an incremental glucose uptake that did not occur in the same animal during a 45-min sham-exposure period. Field exposure using a 50% duty cycle resulted in activation of a 13-mm³ region in the hindbrain (Figs. 1 and 2), as expected (Frilot et al., 2009). When the rats were exposed using a 100% duty cycle, only two evoked potentials were triggered corresponding to the onset of the field and its offset 45 min later; consequently the only meaningful stimulus was the presence of the magnetic field. Increased activation was detected (Figs. 3 and 4), but it involved a brain volume only 27% of that involved in mediating the effect due to the three combined stimuli associated with a 50% duty-cycle (onset, offset, and steady-state responses). The steady-state stimulus was applied continuously for 45 min compared with about 13 min (2 s per 7-s trial) during the 50% duty-cycle condition. The observation of less activation despite the large increase in the duration of the steady-state stimulus suggested that the increased glucose utilization observed under the 50% condition was probably due to the transient stimuli (evoked potentials). Because of the general phenom-

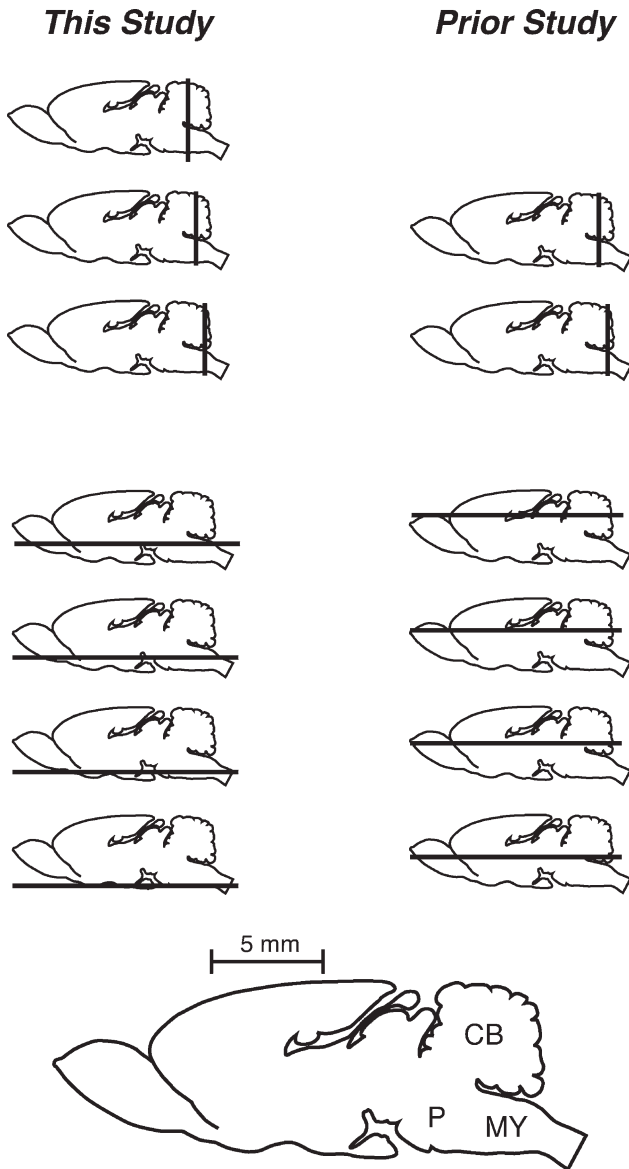


Fig. 6. Comparison of locations of coronal (top) and transverse (bottom) planes containing voxels activated by exposure to a magnetic field having a 50% duty cycle. First column, this study (Figs. 2 and 3); second column, a prior study (Frilot et al., 2009). CB, cerebellum; P, pons. MY, medulla.

enon of adaptation, somatic stimuli, light, sound, touch as examples, usually produce a greater change in brain electrical activity compared with that due to the simple presence of the stimulus in the subject's environment. The larger region of brain activation in the first experiment is therefore consistent with the electrophysiological results.

According to physical law, magnetic fields induce electric fields in the body. We previously proposed a mechanism for transducing the electric field in which the field exerted a force on negatively charged oligosaccharide side chains bound to an ion-channel gate,

thereby mechanically opening the gate (Marino et al., 2009) (Fig. 5). The sensitivity of the process depends on the strength of the field and the effective size of the glycocalyx region that interacts with the field; a region with a radius of about 9 μm can detect a field of 100 $\mu\text{V/m}$, which is near the limit of detectability demonstrated by lower life forms (Kolomytkin et al., 2007). As illustrated (Fig. 5), the optimal direction of the field is orthogonal to the membrane surface. In actuality the optimal direction will depend on the structural characteristics of the glycocalyx, the details of which are generally unknown. Nevertheless the proposed mechanism implies that the local direction of the field at the cell membrane is a critical factor in the transduction process. We reasoned that randomizing the direction of the field would reduce FDG uptake by mitigating the cumulative effect of the field on the ion-channel gate. In our second experiment, where the rats were free to move in the cage, we found that the resulting field randomization eliminated the hindbrain activation observed when the rats were constrained. The results of the second experiment therefore supported our biophysical theory of transduction, although there may be other explanations for why brain activation was not seen in the second experiment.

We showed earlier that the evoked potentials occurred within about 500 ms after presentation of the stimulus (Frilot et al., 2009), and that electroreception in humans and animals occurs in the head (Carrubba et al., 2007; Marino et al., 2003). The results are consistent with the theory that the electroreceptors were located in the hindbrain, where the PET-activated region was found. But biological tissue is essentially transparent to magnetic fields. Consequently the electroreceptor cell (the cell that transduces the EMF) could have been located elsewhere; in this case the activated region in the hindbrain reflected early postprocessing of the afferent signal triggered by transduction.

The PET images were insufficiently detailed to permit direct identification of the activated voxels in specific regions of the brain. Consequently neuroanatomical localization was accomplished by superimposing the emission data on a published atlas of MR images of the rat brain. When we performed this localization process previously, we located the activated voxels in the cerebellum (Frilot et al., 2009). In this study they were located several mm lower in the hindbrain, in the region of the medulla (Fig. 6). There was an inherent error of about 2.3 mm in localizing the activated voxels using our method, which could explain the difference in hindbrain localization between the two studies (Fig. 6). The inherent placement error may also have been responsible for the off-center location of the PET-activated region (Fig. 1). The centroid of the region was 1.69 mm from the hindbrain centerline, and therefore within the error range.

REFERENCES

- Carrubba S, Frilot C, Chesson AL Jr, Marino AA. 2007. Evidence of a nonlinear human magnetic sense. *Neuroscience* 144:356–367.
- Frilot II C, Carrubba S, Marino AA. 2009. Magnetosensory function in rats: Localization using positron emission tomography. *Synapse* 63:421–428.
- Kolomytkin OV, Dunn S, Hart FX, Frilot C, Kolomytkin D, Marino AA. 2007. Glycoproteins bound to ion channels mediate detection of electric fields: A proposed mechanism and supporting evidence. *Bioelectromagnetics* 28:379–385.
- Marino AA, Carrubba S, Frilot C, Chesson AL Jr. 2009. Evidence that transduction of electromagnetic field is mediated by a force receptor. *Neurosci Lett* 452:119–123.
- Marino AA, Carrubba S, Frilot C II, Chesson AL Jr, Gonzalez-Toledo E. 2010. Simulated MR magnetic field induces steady-state changes in brain dynamics: Implications for interpretation of functional MR studies. *Magn Reson Med* 64:349–357.
- Marino AA, Nilsen E, Frilot C. 2003. Localization of electroreceptive function in rabbits. *Physiol Behav* 79:803–810.
- Pizzagalli DA, Oakes TR, Davidson RJ. 2003. Coupling of theta activity and glucose metabolism in the human rostral anterior cingulate cortex: An EEG/PET study of normal and depressed subjects. *Psychophysiology* 40:939–949.
- Pratt H, Starr A, Michalewski HJ, Bleich N, Mittelman N. 2008. The auditory P₅₀ component to onset and offset of sound. *Clin Neurophysiol* 119:376–387.
- Schweinhart P, Fransson P, Olson L, Spenger C, Andersson JLR. 2003. A template for spatial normalisation of MR images of the rat brain. *J Neurosci Meth* 129:105–113.
- Shimoji K, Ravasi L, Schmidt K, Soto-Montenegro ML, Esaki T, Seidel J, Jagoda E, Sokoloff L, Green MV, Eckelman WC. 2004. Measurement of cerebral glucose metabolic rates in the anesthetized rat by dynamic scanning with ¹⁸F-FDG, the ATLAS small animal PET scanner, and arterial blood sampling. *J Nucl Med* 45:665–672.
- Worsley KJ, Evans AC, Marrett S, Neelin P. 1992. A three-dimensional statistical analysis for CBF activation studies in human brain. *J Cereb Blood Flow Metab* 12:900–918.
- Yamashiro K, Inui K, Otsuru N, Kida T, Kagigi R. 2009. Somatosensory off-response in humans: An MEG study. *Neuroimage* 44:1363–1368.